Composites: Part B 56 (2014) 413–423

Contents lists available at ScienceDirect

Composites: Part B

journal homepage: www.elsevier.com/locate/compositesb

Strain assisted diffusion: Modeling and simulation of deformation-dependent diffusion in composite media

D. Klepach [b,*], T.I. Zohdi [a]

[a] Department of Mechanical Engineering, University of California, 6195 Etcheverry Hall, Berkeley, CA 94720-1740, USA
[b] Department of Mechanical Engineering, University of California, 6102 Etcheverry Hall, Berkeley, CA, USA

ARTICLE INFO

Article history:
Received 31 January 2013
Accepted 12 August 2013
Available online 22 August 2013

Keywords:
A. Carbon fiber
B. Wettability
C. Analytical modeling
C. Computational modeling
Diffusion

ABSTRACT

In this work, we develop a model for strongly-coupled, deformation-dependent diffusion in composite media at finite strains. The coupling incorporates the effects of deformation into the diffusivity tensor. A time-transient, three-dimensional variational formulation is developed and then discretized using the Finite Element Method in conjunction with an implicit staggering scheme to resolve the coupled multiphysics. Numerical examples are provided to illustrate the model.

1. Introduction

In many modern engineering applications, diffusion in solids plays a major role in the operation of devices which are, in many cases, constructed from composite media. As a species diffuses into a solid, a complex physical process occurs, which primarily manifests itself as macroscopic swelling. The diffusion process can have a major effect on the operation resulting in large deformations and stresses and, in some cases, failure. In this paper, we investigate the phenomena of strong coupling between diffusion of a species into a nonlinear elastic solid body and the concentration, deformation, and stresses in that body. We are particularly interested in fiber-reinforced composite materials with different mechanical and diffusive properties. We consider cases where the diffusion and deformation are coupled in both directions, i.e. they affect one another. We first investigate the qualitative behavior analytically, then the time-transient, three-dimensional behavior for composite systems by developing a variational formulation which is then discretized using the Finite Element Method, in conjunction with an implicit staggering scheme.

Specifically, in this study we construct mathematical models where we begin with the separate, well-established, models for diffusion and finite elasticity. For diffusion, we consider enhancements to Fick's laws of diffusion. For elasticity, we consider a moderate finite strain elastic model employing a Kirchhoff–Saint Venant material. We consider material constants to be coupled and consider strain-dependent diffusivity, where the diffusivity tensor depends on the volumetric strain through the Jacobian $J = det(\boldsymbol{F})$. We also consider saturation effects, where a finite amount of diffusing species is absorbed by the solid and the diffusion process terminates. This is modeled as having a diffusivity tensor that is dependent on species concentration.[1] Early work on the coupling of diffusion and deformation or stress was done by Truesdell [1] Green and Adkins [2], and Adkins [3,4] have made major advancements in the field. Later on, Aifantis et al. [5–7] did work on stress-assisted diffusion, and also *Mixture theory* was used to model the coupling by Rajagopal [8]. In the last decade or so, there were recent theoretical advancements in nonlinear diffusion and mechanics that we found to be most relevant to this study. Baek and Srinivasa [9] came up with a more direct approach that deals with the problem and compared it with mixture theory, finding both theories to be comparable. Suo et al. analyzed large deformations in gels [10], which was useful in the development of the present model. For more complex modeling, including damage and thermal effects, see Zohdi [11] and Duda et al. [12].

2. Modeling deformation-dependent diffusion

We establish the basic settings of this model in the reference configuration. Capital letters are associated with the reference configuration and lower-case letters are associated with the current configuration. Letters with a tilde ($\tilde{\square}$) are associated with diffusive

* Corresponding author. Tel.: +1 972538237381.
E-mail address: klepachd@berkeley.edu (D. Klepach).

[1] For example, one could describe this by specifying that above a certain level of concentration the values of diffusivity tensor would drop to zero.

1359-8368/$ - see front matter © 2013 Elsevier Ltd. All rights reserved.
http://dx.doi.org/10.1016/j.compositesb.2013.08.035

processes, and the letters without any sign are mechanical variables. For three dimensional diffusion, the most common constitutive laws are known as Fick's laws, where the flux is related to the gradient of the concentration of a substance, $\widetilde{C}$, at a material point as,

$$\widetilde{\mathbf{J}} = -\widetilde{\mathbf{D}} Grad(\widetilde{C}). \tag{1}$$

where $\widetilde{\mathbf{D}}$ is the diffusivity tensor. Conservation of mass in a material point with no internal source terms can be written,

$$\frac{\partial \widetilde{C}}{\partial t} = -Div(\widetilde{\mathbf{J}}), \tag{2}$$

where *Div* is the divergence operator with respect to the reference configuration. Combining the two Eqs. (1), (2) yields

$$\frac{\partial \widetilde{C}}{\partial t} = Div(\widetilde{\mathbf{D}} Grad(\widetilde{C})) \tag{3}$$

which is known as Fick's law of diffusion. For mechanics, we use the balance of linear momentum

$$Div(\mathbf{P}) + \rho_{ref}\mathbf{f}_{ref} = \rho_{ref}\ddot{\mathbf{u}}_{ref} \tag{4}$$

where $\mathbf{P}$ is the first Piola–Kirchhoff stress, $()_{ref}$ implies the reference configuration, ρ is the mass density,$\mathbf{f}$ are the body forces, and $\ddot{\mathbf{u}}_{ref}$ is the second time derivative of the displacement. For elasticity, we consider a Kirchhoff–Saint Venant nonlinear elastic material model

$$\mathbf{S} = \mathbb{E} : \mathbf{E} \tag{5}$$

where $\mathbf{S}$ is the Second Piola–Kirchhoff stress and $\mathbf{E} = \frac{1}{2}(\mathbf{C} - \mathbf{I})$ is the Green–Lagrange strain tensor. We define the strains due to diffusion as $\mathbf{E}_c$, and consider the diffusion tensor, $\widetilde{\mathbf{D}}$, to be a function of the mechanical deformation and the concentration as,

$$\widetilde{\mathbf{D}} = \widetilde{\mathbf{D}}(\mathbf{E}, \widetilde{C}). \tag{6}$$

This allows us to construct mathematical models which describe different physical phenomena. The modified Second Piola–Kirchhoff stress becomes

$$\mathbf{S} = \mathbb{E} : (\mathbf{E} - \mathbf{E}_c) \tag{7}$$

and the modified diffusion equation becomes

$$\frac{\partial \widetilde{C}}{\partial t} = Div(\widetilde{\mathbf{D}}(\mathbf{E}, \widetilde{C}) Grad(\widetilde{C})) \tag{8}$$

where *Grad* is the gradient operator with respect to the reference configuration.

3. Strain-dependent diffusivity

We assume that the diffusivity tensor, $\widetilde{\mathbf{D}}$, is a function of the deformation in general, and specifically a function of the volume change through the Jacobian as

$$\widetilde{\mathbf{D}} = \widetilde{\mathbf{D}}(J). \tag{9}$$

Some simple arguements provide guidance on constructing a model for $\widetilde{\mathbf{D}}(J)$. For example, if we continuously compress the material, it is reasonable to assume that the diffusivity will decrease to a lower limit (becoming fully densified), which we will take to be equivalent to zero diffusivity. As the volume increases, the magnitude of the diffusivity will grow to values larger than of the reference configuration ($J > 1$). In terms of a function, we require that $\widetilde{\mathbf{D}}(J = 0) = \mathbf{0}$, $\widetilde{\mathbf{D}}(J = 1) = \widetilde{\mathbf{D}}_0$. The actual values are material dependent, and can be found experimentally. We also assume that the function is smooth and continuous. A function that satisfies these requirements is the following:

$$\widetilde{\mathbf{D}}(J) = \widetilde{\mathbf{D}}_0 \frac{e^{aJ} - 1}{e^a - 1} \tag{10}$$

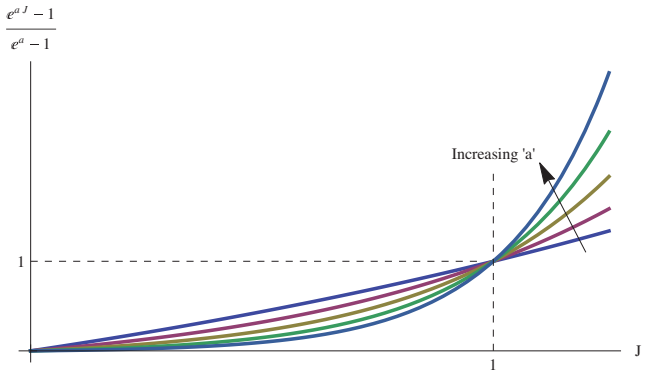

Fig. 1. Volume dependent diffusivity.

where 'a' is a constant that is determined experimentally. For the case where there are no deformations, the diffusivity tensor scales to its initial value $\widetilde{\mathbf{D}}_0$. The plot for Eq. (10) can be seen in Fig. 1.

4. Swelling strains

We now consider some simple models for swelling strains (i.e. $J > 1$).

4.1. Uniform swelling

In the simplest case, similar to thermo-elasticity, we consider uniform (isotropic, or direction-independent swelling, i.e. see [11]) defined via

$$\mathbf{E}_C = \beta(\widetilde{C} - \widetilde{C}_0)\mathbf{I} \tag{11}$$

where $\widetilde{C}_0$ is a material initial concentration and β is a scalr material constant that controls the magnitude of the stress resulting from the swelling (similar to the coefficient of volumetric thermal expansion, α_κ, in thermo-elasticity). This yields the Second Piola–Kirchoff stress as

$$\mathbf{S} = \mathbb{E} : (\mathbf{E} - \beta(\widetilde{C} - \widetilde{C}_0)\mathbf{I}). \tag{12}$$

4.2. Non-uniform swelling

Alternatively, one may assume that the solid swells up non-uniformly (i.e anisotropic, or directionally-dependent). Specifically, it has preferred directions in which it will swell (i.e. along the direction of material fibers). We define β as a material constant, and $\mathbf{M}$ is a unit vector normal to the plane of isotropy in the reference configuration (i.e. $\mathbf{M}$ is in the direction of the fibers in a fiber-composite material). We assume that the material will swell up in any direction normal to the fiber direction, thus we use the projection tensor $\mathbf{I} - \mathbf{M} \otimes \mathbf{M}$. With that, we define the stress as,

$$\mathbf{S} = \mathbb{E} : [\mathbf{E} - \beta(\widetilde{C} - \widetilde{C}_0)(\mathbf{I} - \mathbf{M} \otimes \mathbf{M})] \tag{13}$$

Remark. As mentioned earlier, beyond a certain concentration level $\widetilde{C}_1$ (which is a material constant), the diffusivity is set to zero so that the diffusion process is terminated. Below a certain concentration level $\widetilde{C}_0$ (again, a material constant) it should initially retain its initial value of $\widetilde{D}_0$. In the range $[\widetilde{C}_0, \widetilde{C}_1]$ smoothly, we define the diffusivity as

$$\widetilde{D}(\widetilde{C}) = \widetilde{D}_0 - (\widetilde{D}_0 - \widetilde{D}_1) / \left(exp\left(\frac{\frac{\widetilde{C}_0 + \widetilde{C}_1}{2} - \widetilde{C}}{\alpha} \right) + 1 \right) \tag{14}$$

where $\widetilde{D}_1$ can be set to zero for full saturation. α is a non-dimensional material constant smoothing factor that controls the rate of change of the diffusivity with respect to the concentration with in the range $[\widetilde{C}_0, \widetilde{C}_1]$. It is set to be greater than zero ($\alpha > 0$), as zero is a limiting case that causes a jump in the diffusivity from $\widetilde{D}_0$ to $\widetilde{D}_1$. The affects of α, and the general behavior of the function can be seen in Fig. 2.

5. Finite element formulation

In order to computationally investigate and analyze the model, we provide a concise *Finite Element* formulation.

5.1. Balance of linear momentum

Starting with the local equation in the reference configuration, we have

$$Div(\mathbf{P}) + \rho_{ref}\mathbf{f}_{ref} = \rho_{ref}\ddot{\mathbf{u}}_{ref} \tag{15}$$

We apply an inner product with a vector test function $\mathbf{v}$, and integrate over the entire reference region Ω_0, to get

$$\int_{\Omega_0} [\mathbf{v}\cdot Div(\mathbf{P}) + \rho_{ref}\mathbf{v}\cdot\mathbf{f}_{ref}]d\Omega_0 = \int_{\Omega_0}\rho_{ref}\mathbf{v}\cdot\ddot{\mathbf{u}}_{ref}d\Omega_0 \tag{16}$$

We apply the product rule and the *Divergence theorem*, and invoke that on the boundary wherever the displacement is known (Γ_u) the test function $\mathbf{v}$ is set to be zero. From that we and get the weak form of Eq. (15)

$$\int_{\Gamma_p}\mathbf{v}\cdot\mathbf{p}d\Gamma_p - \int_{\Omega_0} Grad(\mathbf{v})\cdot\mathbf{P}d\Omega_0 + \int_{\Omega_0}\rho_{ref}\mathbf{v}\cdot\mathbf{f}_{ref}d\Omega_0 = \int_{\Omega_0}\rho_{ref}\mathbf{v}\cdot\ddot{\mathbf{u}}_{ref}d\Omega_0 \tag{17}$$

where $\mathbf{p} = \mathbf{P}\cdot\mathbf{N}$ is the Piola traction in the reference configuration, Γ_p is the boundary where the tractions are specified, and $\partial\Omega_0 = \Gamma_p \cup \Gamma_u$. The solution of this equation can be approximated with the use of the *Finite Element* method and *time discretization*. With the use of the *Backward Euler* time-scheme and following the Galerkin procedure, for the righthand side of the equation we obtain

$$\mathbf{b}\left[\frac{1}{\Delta t_L^2}\mathbf{M}^{L+1}\mathbf{a}^{L+1} - \frac{1}{\Delta t_L}\left(\frac{1}{\Delta t_L}+\frac{1}{\Delta_{L-1}}\right)\mathbf{M}^{L}\mathbf{a}^{L} + \frac{1}{\Delta t_L\Delta_{L-1}}\mathbf{M}^{L-1}\mathbf{a}^{L-1}\right] \tag{18}$$

where $\mathbf{M}^L$ is known as the mass matrix at time L, Δt_L is the time-step at time L, $\mathbf{b}$ are arbitrary constants, and $\mathbf{a}^L$ are the displacements at time L. For the lefthand side of Eq. (17), we obtain

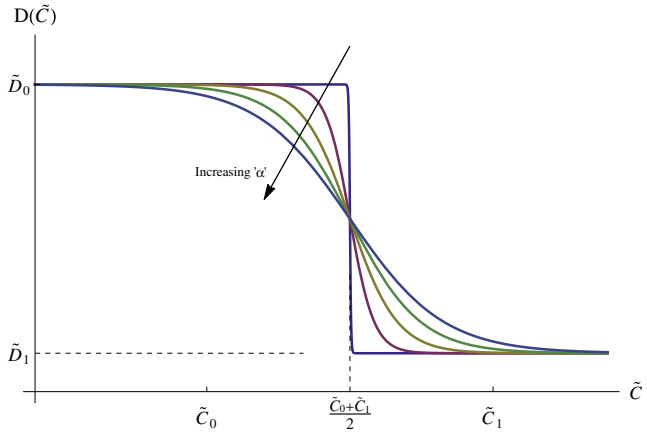

Fig. 2. Diffusivity for saturation.

$$\mathbf{b}\left[\int_{\Gamma_p}\mathbf{p}_\phi d\Gamma_p - \int_{\Omega_0}\mathbf{D}[\phi]\mathbf{P}d\Omega_0 + \int_{\Omega_0}\rho_{ref}\mathbf{f}_\phi^{ref}d\Omega_0\right] \tag{19}$$

where $\mathbf{p}_\phi$ is related to $\mathbf{p}$, $\mathbf{D}[\phi]$ is a derivative operator, and $\mathbf{f}_\phi^{ref}$ is related to $\mathbf{f}_{ref}$. This leads to the discrete form of the balance of linear momentum, and since $\mathbf{b}$ is arbitrary we get

$$\mathbf{a}^{L+1} = \Delta t_L^2[\mathbf{M}^{L+1}]^{-1}(\mathbf{f}^{ext} + \mathbf{f}^{int}) \tag{20}$$

where

$$\mathbf{f}^{ext} = \int_{\Gamma_p}\mathbf{p}_\phi d\Gamma_p + \int_{\Omega_0}\rho_{ref}\mathbf{f}_\phi^{ref}d\Omega_0 \tag{21}$$

and

$$\mathbf{f}^{int} = -\int_{\Omega_0}\mathbf{D}[\phi]\mathbf{P}d\Omega_0 + \left[\frac{1}{\Delta t_L}\left(\frac{1}{\Delta t_L}+\frac{1}{\Delta t_{L-1}}\right)\mathbf{M}^L\mathbf{a}^L - \frac{1}{\Delta t_L\Delta t_{L-1}}\mathbf{M}^{L-1}\mathbf{a}^{L-1}\right] \tag{22}$$

5.2. Diffusion equation

Starting with the diffusion equation in the reference configuration, we have

$$\frac{\partial\widetilde{C}}{\partial t} = Div(\widetilde{\mathbf{D}}Grad(\widetilde{C})) \tag{23}$$

We apply an inner product operation with a scalar test function v on both sides of the equation, and integrate over the entire reference region Ω_0 to get

$$\int_{\Omega_0} v\frac{\partial\widetilde{C}}{\partial t}d\Omega_0 = \int_{\Omega_0} vDiv(\widetilde{\mathbf{D}}Grad(\widetilde{C}))d\Omega_0. \tag{24}$$

We use the *product rule* and the *Divergence theorem*, and invoke that on the boundary wherever the concentration is known ($\Gamma_{\widetilde{C}}$) the test function v is set to be zero to get the weak form of Eq. (23)

$$\int_{\Omega_0} v\frac{\partial\widetilde{C}}{\partial t}d\Omega_0 = \int_{\Gamma_{\widetilde{J}}} v\widetilde{\mathbf{J}}\cdot\mathbf{N}d\Gamma_{\widetilde{J}} - \int_{\Omega_0} Grad(v)\cdot\widetilde{\mathbf{D}}\cdot Grad(\widetilde{C})d\Omega_0 \tag{25}$$

where $\Gamma_{\widetilde{J}}$ is the boundary where the flux is prescribed, and $\partial\Omega_0 = \Gamma_{\widetilde{J}} \cup \Gamma_{\widetilde{C}}$. The solution of this equation can be approximated with the use of the *Finite Element* method and *time discretization*. With the use of the *Backward Euler* time-scheme we follow the Galerkin procedure and approximate the concentration and the test function to obtain

$$\mathbf{b}\frac{1}{\Delta t_L}\mathbf{M}^c(\mathbf{c}^{L+1} - \mathbf{c}^L) = \mathbf{b}\left[\int_{\Gamma_{\widetilde{J}}}\widetilde{\mathbf{J}}_\phi d\Gamma_p - \int_{\Omega_0}\mathbf{D}[\phi]\widetilde{\mathbf{D}}\cdot Grad(\widetilde{C})d\Omega_0\right] \tag{26}$$

where $\mathbf{M}^c$ is known as the mass matrix and $\mathbf{c}^L$ are the discrete concentrations at time L. Δt_L is the time step at time L, $\mathbf{b}$ are arbitrary constants, $\widetilde{\mathbf{J}}_\phi$ is related to the flux $\mathbf{J}$, and $\mathbf{D}[\phi]$ is a derivative operator. Since $\mathbf{b}$ is arbitrary we get the following

$$\mathbf{c}^{L+1} = \mathbf{c}^L + \Delta t_L[\mathbf{M}]^{-1}\left[\int_{\Gamma_{\widetilde{J}}}\widetilde{\mathbf{J}}_\phi d\Gamma_p - \int_{\Omega_0}\mathbf{D}[\phi]\mathbf{D}\cdot Grad(\widetilde{C})d\Omega_0\right] \tag{27}$$

Table 1
Cases of modeling the coupling of deformation-dependent diffusion.

Case #	Eqn.	Desription	Material const.
Case 1		Fixed diffusivity	$\widetilde{\mathbf{D}}_0, \beta, \widetilde{C}_0, \mathbb{E}_0$
Case 2	(10)	Strain dependent diffusivity	$\widetilde{\mathbf{D}}_0, \beta, \widetilde{C}_0, a, \mathbb{E}_0$
Case 3	(13)	Saturation	$\widetilde{\mathbf{D}}_0, \widetilde{\mathbf{D}}_1, \beta, \widetilde{C}_0, \widetilde{C}_1, \alpha, \mathbb{E}_0$
Case 4	(14)	Diffusion induced nonuniform strain	$\widetilde{\mathbf{D}}_0, \beta, \widetilde{C}_0, \mathbf{M}, \mathbb{E}_0$

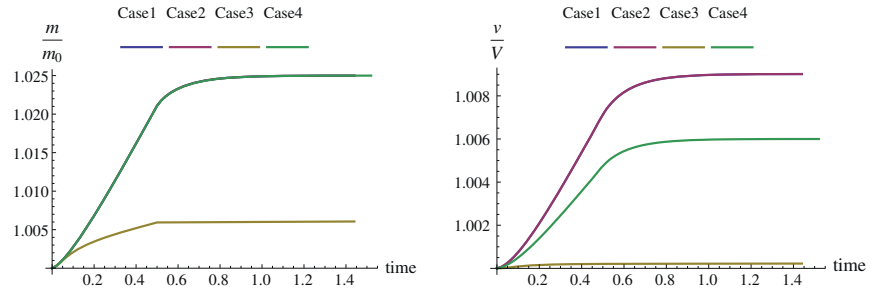

Fig. 3. Plots of the nondimensional mass and volume as functions of time.

6. Staggering scheme

With the *Finite Element* formulation set up, a numerical solver needs to be prescribed in order to solve the coupled equations. We introduce here the details of the staggering scheme that was used in the computational modeling of the equations.

6.1. Fixed point iteration

Since the equations are nonlinear, a nonlinear solver is required. We used *Fixed Point Iteration*, that even though it has a lower order of convergence compared to Newton's method, it is known to be advantageous for finding solutions to problems involving stability or multi-field coupled problems where the variables are of different order of magnitude. Constructing a *Fixed Point Iteration* scheme does not require a stiffness matrix (required for Newton's method), which can be ill conditioned due to different orders of magnitude in the coupled equations (i.e. elasticity and diffusion). The method iterates the already specified equations until convergence.

Algorithm 1. Algorithm for fixed point iterations

Guess an initial solution $x = x_0$
Set $i = 1$
while $\|f(x_i)\| > TOL$ **do**
  1. $x_{i+1} = f(x_i)$
  2. $i = i + 1$
end while

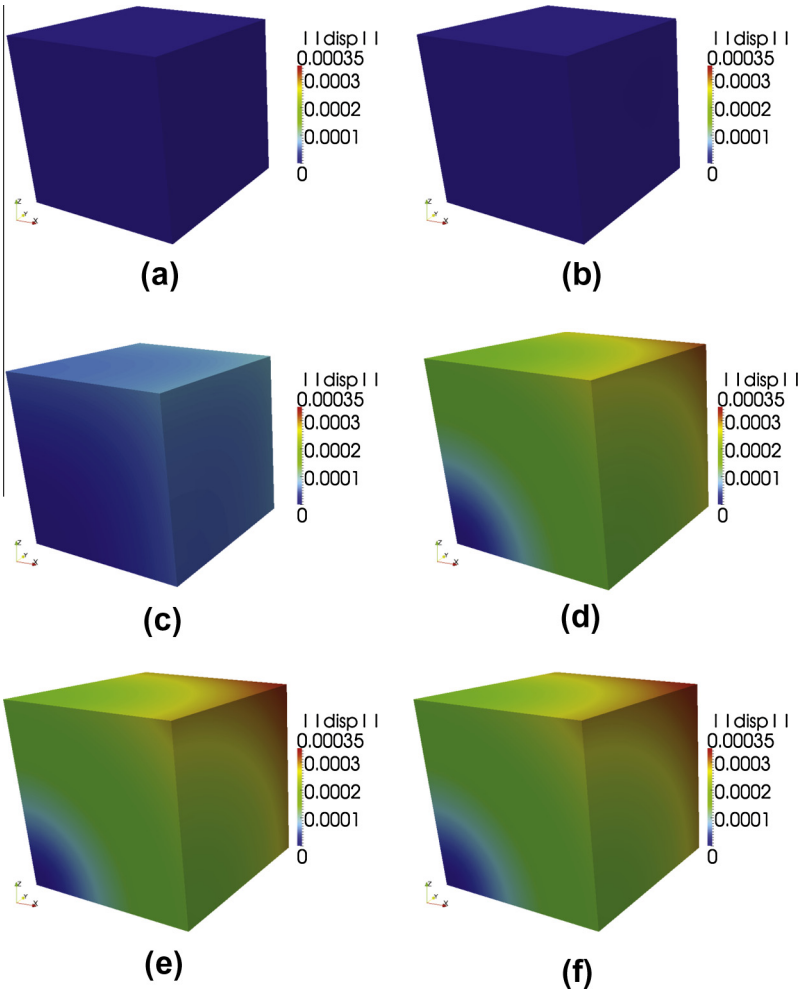

Fig. 4. Plots of the magnitude of the displacement case 2 at different time steps (displacements are magnified by a factor of 50). *Note*: only one eighth of the cube is plotted.

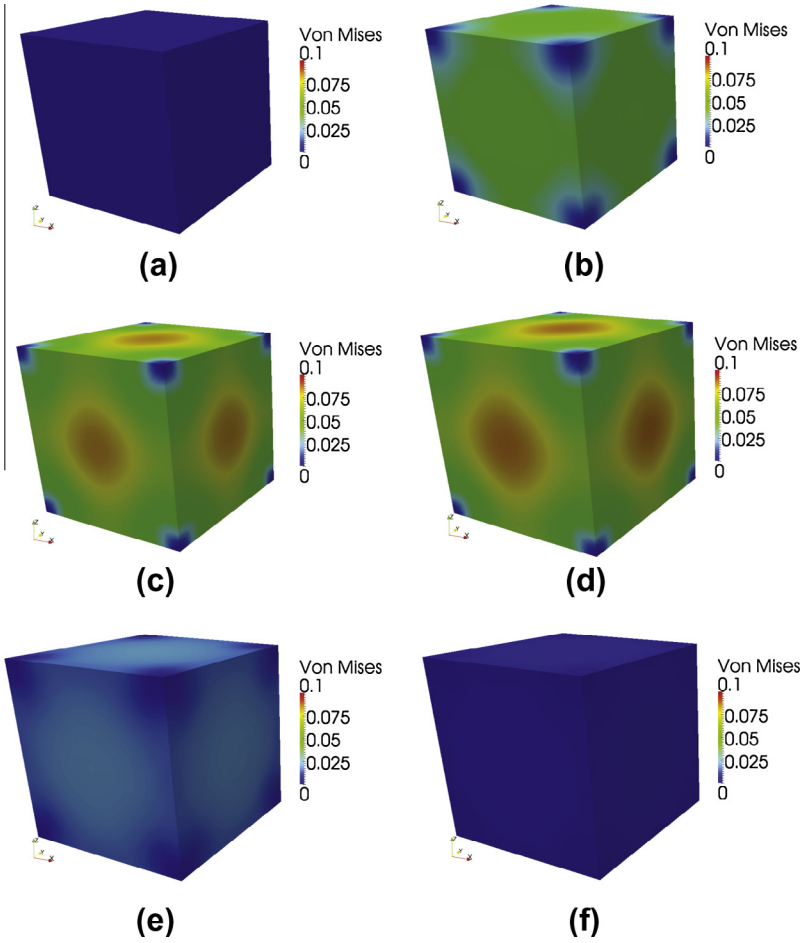

Fig. 5. Plots of the Von Mises stress at different time steps for case 2 strain dependent diffusivity.

Given an equation of the form $x = f(x)$, the algorithm for the method is as follows:

The conditions for the method to hold (to converge) are known as the *Lipschitz condition* (explained in [13,14]).

6.2. The staggering method

This method can be generalized for N equations, but, for simplicity we show it for two equations, and for the case most suitable for our computations (i.e. it suitable for fixed point iteration).

Given two variables x and y, and two equations that depend on those variables $x = f(x,y)$ and $y = g(x,y)$, the algorithm for the method is as follows:

Algorithm 2. Algorithm for fixed point iterations

Set $i = 1$, $Norm_x = Norm_y = 10^{10}$ (large number)
Guess an initial solution $x_i = x_0$, $y_i = y_0$
while $\|Norm_x\| > TOL_x$ or $\|Norm_y\| > TOL_y$ **do**
1. $x_{i+1} = f(x_i, y_i)$
2. $Norm_x = \|x_i - x_{i+1}\|$
3. $x_i = x_{i+1}$
4. $y_{i+1} = g(x_i, y_i)$
5. $Norm_y = \|y_i - y_{i+1}\|$
6. $y_i = y_{i+1}$

end while

These two methods comprise our scheme for solving the coupled, nonlinear algebraic equations.

7. Numerical examples

With the combined numerical scheme in hand, we use it to simulate and analyze different model problems. Table 1 ilustrates the different cases.

We consider the case of free swelling (traction-free boundary constraints) where the body is subjected to a change in the concentration on all the boundaries, and due to the diffusion into the body, it will swell. Specifically, the concentration boundary conditions are set as follows: the body has an initial concentration $\widetilde{C}_0$ in the entire body at time $t = 0$. For a short amount of time up to $t = t_r$ the concentration on the boundary is linearly ramped up to a value of $\widetilde{C}_f$, and it is kept at that value until the end of the simulation at time $t = t_f$. This mimics a solid with an initial concentration submerged into a infinite bath with a different concentration.

As a first example, we study a fiber-free material, i.e only the matrix. Afterwards, we study a matrix material with embedded fibers. Three cases are considered: strain dependent diffusivity, saturation, and diffusion induced nonuniform strain. For comparison, the same loads, boundary and initial conditions are applied in all cases. For the matrix we chose a standard Epoxy resin ($E = 5$ GPa, $\nu = 0.30$, $\rho = 1200\ \frac{kg}{m^3}$, $\widetilde{D} = 0.010\ \frac{m^2}{s}$, $\widetilde{D}_{max} = 0.010\ \frac{m^2}{s}$, $\widetilde{D}_{min} = 0.0\ \frac{m^2}{s}$, $\widetilde{C}_0 = 46.0\ \frac{kg}{m^3}$, $\widetilde{C}_1 = 60.0\ \frac{kg}{m^3}$, $\alpha = 0.80$, $\beta = 0.00010\ \frac{m^3}{kg}$), and for the fibers we chose carbon-fibers

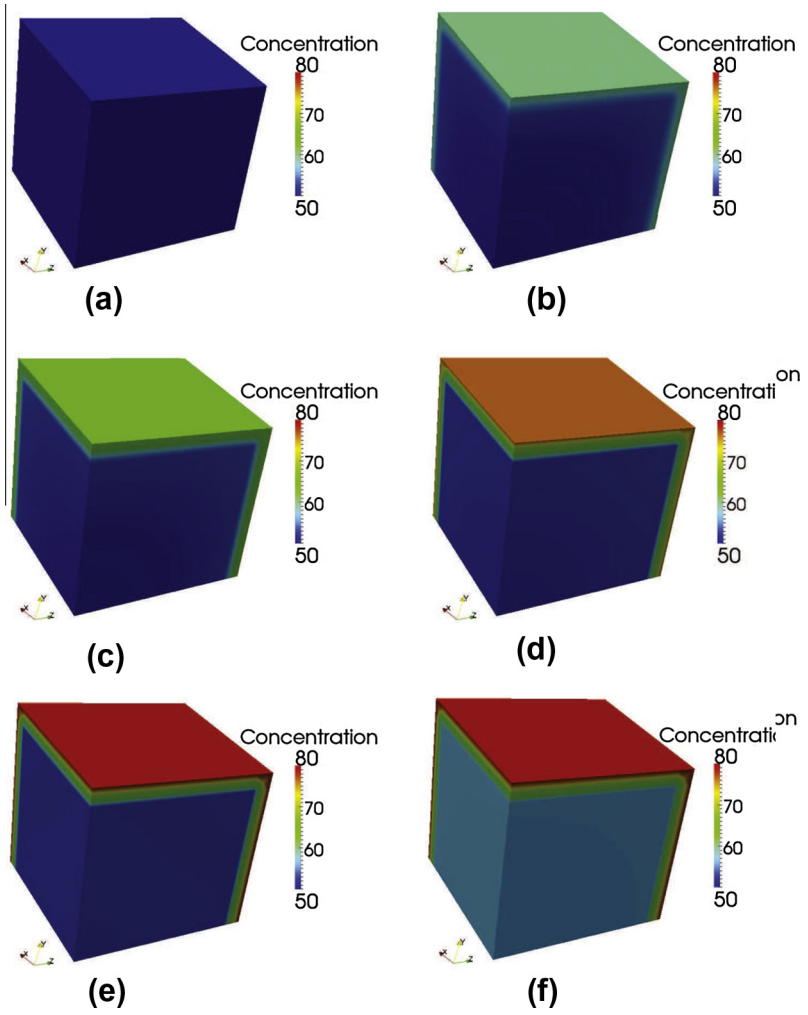

Fig. 6. Plots of the concentration in case 3 (saturation) at different time steps. *Note*: only one eighth of the cube is plotted.

(C_{11}=20 GPa, C_{12}=9.98 GPa, C_{13}=6.45 GPa, C_{33}=235 GPa, C_{44}=24 GPa, $\rho = 1800\ \frac{\text{kg}}{\text{m}^3}$, $\tilde{D} = 0.10\ \frac{\text{m}^2}{\text{s}}$, $\tilde{C}_0 = 50.0\ \frac{\text{kg}}{\text{m}^3}$, $\tilde{C}_1 = 55.0\ \frac{\text{kg}}{\text{m}^3}$, $\alpha = 0.80$, $\beta = 0.00010\ \frac{\text{m}^3}{\text{kg}}$). The matrix was modeled as an isotropic material and the fibers as a transversely isotropic material.

In these examples, of primary interest was the concentration in the body, as well as the Von Mises stress and the displacements. Note that the model for free swelling does not induce stresses in a homogeneous body at steady state, however, transient stresses will be induced during the redistribution of the diffusing phase in the body, as dictated by our model, which relates the stress in the body to the difference between the strains and the strains-due-to-diffusion ($\mathbf{S} = \mathbb{E} : (\mathbf{E} - \mathbf{E}_c)$). As the concentration in the body changes with space and time during the transient phase, the strains due to diffusion, $\mathbf{E}_c$ vary in the body and therefore the stresses as well. As the body reaches steady state, the concentration in the body becomes homogeneous and strains match the strains-due-to-diffusion. The magnitude of the stresses becomes smaller and reaches zero at steady state.

Fig. 3(a) shows the change of nondimensional total mass of the body (current mass divided by initial mass) with respect to time. The plots of cases 1, 2, and 4 are overlaid. The curves rise as the concentration ramps up on the boundaries, and then gradually approach a final value that corresponds to the final level of concentration in the body. For case 3 (saturation), we see that the curve does not rise in a linear manner, it rises to a constant value which is the saturation point of the body. It then remains at that value for the rest of the simulation. Even though on a local level the cases are different, on a global level cases 1, 2, and 4 accumulate mass in the same manner as there are no restrictions such as in case 3. The body absorbs the diffusing matter according to the magnitude of the diffusivity, the boundary and initial conditions (equal in all four cases), which is why case 3 differs in mass accumulation.

Fig. 3(b) shows the change of nondimensional total volume of the body (divided by its initial volume) as a function of time. The plots of cases 1 and 2 are overlaid. For case 3 (saturation), we observe that the curve rises to a constant value which is the saturation point of the body. The saturation point in this case is set low so that in comparison with the other cases the volume in case 3 barely changes. For case 4 (Nonuniform diffusion induced strain) the curve is similar to cases 1 and 2, but the maximum magnitude is smaller. That is due to the fact that the direction of the nonuniformity (vector **M** in the model) constrains the deformations in that direction and therefore the total volume is constrained as well.

In the next few sections a more detailed analysis is shown for cases 2, 3, and 4 where different variables and parameters are displayed as they change in space and time. A block with dimensions of 0.1 m × 0.1 m × 0.1 m is taken to be one eighth of the total size due to the symmetry of the problem.

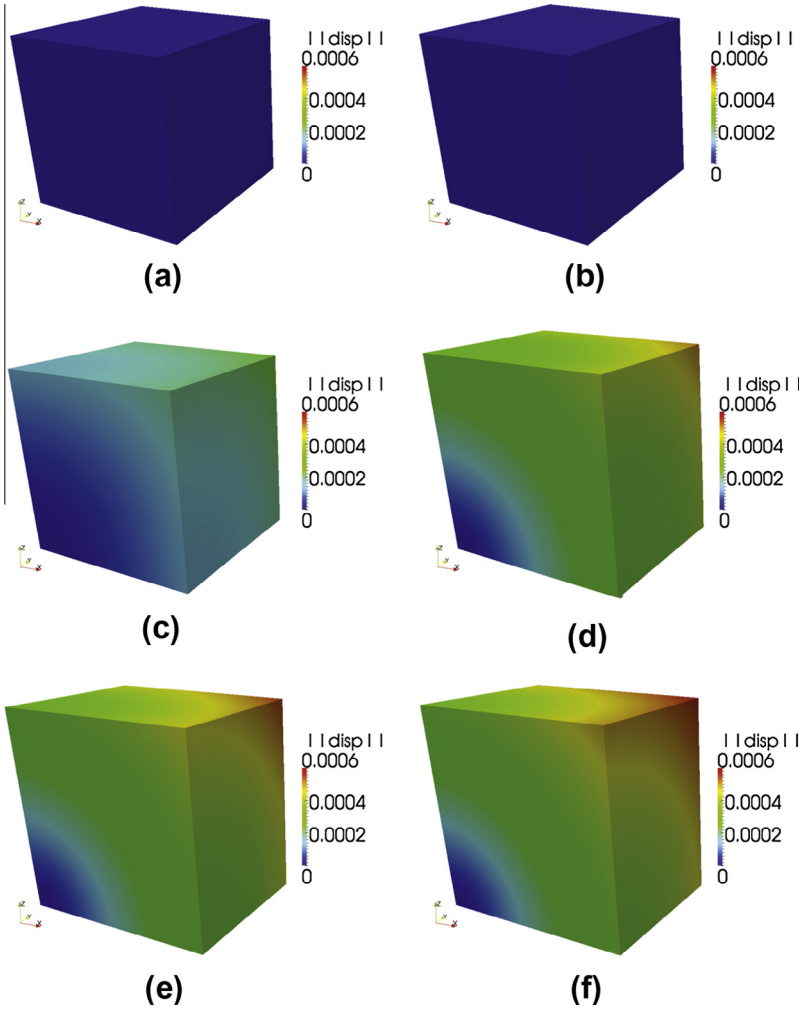

Fig. 7. Plots of the magnitude of the displacement case 4 at different time steps (displacements are magnified by a factor of 50). *Note*: only one eighth of the cube is plotted.

7.1. Case 2: strain dependent diffusivity

Now consider a homogeneous material with the following constitutive models:

$$\widetilde{\mathbf{D}}(J) = \widetilde{\mathbf{D}}_0 \frac{e^J - 1}{e - 1}$$
$$\mathbf{S} = \mathbb{E} : (\mathbf{E} - \beta(\widetilde{C} - \widetilde{C}_0)\mathbf{I}) \tag{28}$$

which accounts for uniform strain-dependent diffusion. Fig. 4 shows the change of magnitude of the displacement during the change of concentration in one eighth of the block. As the concentration is ramped up on the boundaries, the displacements become larger creating spherical iso-surfaces centered in the center of the block. The center of the block does not experience any displacements and the furthest corner from the center displaces the most. This is according to our model that is composed of uniform induced-diffusion and difference between the mechanically-induced-strains and strains-due-to-diffusion.

Fig. 5 shows how the non-dimensional Von Mises stress (divided by the yield stress), change during the change of concentration in the body. The dynamic process of swelling causes both stresses normal and shear stresses in all directions, creating a complex spatial variance in the Von Mises stress. The center of the block remains at zero stress throughout the process, and the furthest corners are able to match the concentrations at the boundaries quickly as well as deform more freely compared to the rest of the block. Because of that, the corners experience zero stress throughout the process as well. At the middle of the faces of the block the surroundings constrain the deformations and the concentration ramp up as this is the boundary. This causes the highest stresses to be in the center of each face and the magnitude of the Von Mises stress, influenced by both the concentration and the deformation, is spatially reduced further away from that point.

7.2. Case 3: saturation

Now consider a homogeneous material with a saturation model for the diffusion process. The following constitutive models are used:

$$\widetilde{\mathbf{D}}(\widetilde{C}) = \widetilde{\mathbf{D}}_0 - \frac{\widetilde{\mathbf{D}}_0}{Exp((\frac{\widetilde{C}_0+\widetilde{C}_1}{2} - \widetilde{C})/\alpha) + 1}$$
$$\mathbf{S} = \mathbb{E} : \left(\mathbf{E} - \beta\left(1 - \frac{1}{Exp\left(\left(-\frac{\widetilde{C}_0+\widetilde{C}_1}{2} + \widetilde{C}\right)/\alpha\right) + 1}\right)\mathbf{I}\right) \tag{29}$$

where $\alpha = 0.80, \widetilde{C}_0 = 46.0$ and $\widetilde{C}_1 = 60.0$ so that the concentration level in saturation is set at $\frac{\widetilde{C}_0+\widetilde{C}_1}{2} = 53$. Fig. 6 shows the changes in concentration in the block. The entire body is with an initial concen-

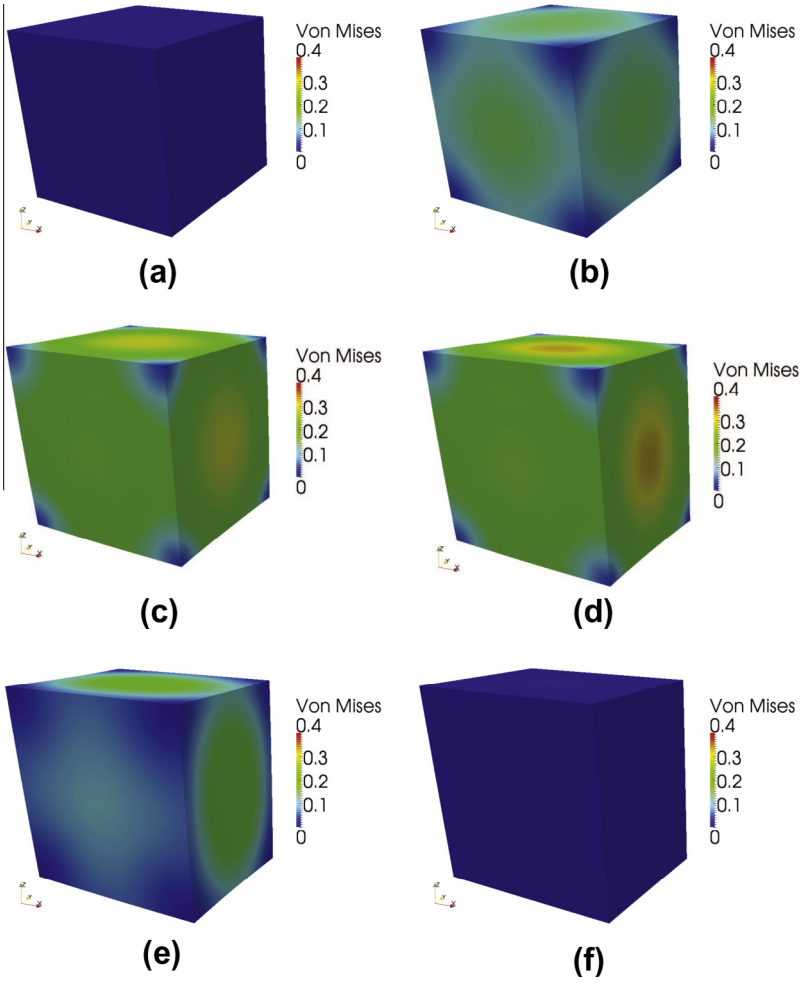

Fig. 8. Plots of the Von Mises stress case 4 at different time steps.

tration of $\widetilde{C} = 50$ which is ramped up on the boundaries up to a magnitude of $\widetilde{C} = 80$. Even though the concentration is ramped up on the boundaries to $\widetilde{C} = 80$, the concentration inside the block never reaches those values. The maximum level of concentration in the body is 53 as prescribed, and there is a high gradient close to the boundaries. This is a numerical artifact which becomes smaller with the size of the elements (the gradient passes through one element satisfying boundary conditions on one end, and saturation condition on the other). At steady state, although the gradient is large, the stresses are reduced to zero.

7.3. Case 4: diffusion induced nonuniform strain

Finally, we consider a homogeneous material with nonuniform strain induce by diffusion. The following constitutive models are used:

$$\begin{aligned} \widetilde{\mathbf{D}} &= \widetilde{\mathbf{D}}_0 \\ \mathbf{S} &= \mathbb{E} : (\mathbf{E} - \beta(\widetilde{C} - \widetilde{C}_0)(\mathbf{I} - \mathbf{M} \otimes \mathbf{M})) \end{aligned} \tag{30}$$

where $\mathbf{M}$ is set normal to one of the face in the block. Fig. 7 shows how the magnitude of the displacement change during the change of concentration in the block. Due to the nonuniform deformation, induced by diffusion, the maximum magnitude of the displacements in this case is almost twice as large as the values shown in case 2. Because this is a homogeneous material, in steady-state the stresses die down and the body has a homogeneous distribution of the concentration. Since the model has nonuniform strains-induced-by-diffusion, even though the material is isotropic, we see that the iso-surfaces constructed by constant values of Von Mises stress are ellipsoidal and not spherical, as expected. The body swells up and deforms due to diffusion in two main directions, causing it to deform in the third direction due to Poisson's effect.

Fig. 8 shows how the non-dimensional Von Mises stress (divided by the yield stress), change during the change of concentration in the body. It is evident that the stress evolves in a different manner than that shown in case 2, as the magnitude of the stress in the direction of $\mathbf{M}$ is much smaller compared to the other faces. The overall magnitude of the stress is four times higher than in case 2, indicating that even though the parameters for the uniform and nonuniform cases are the same the non-uniformity plays a major role in producing stresses.

7.4. Free swelling of a fiber composite material

We consider a fiber composite material where the matrix and the fibers have different mechanical and diffusivity properties (stated above). These differences create a complex behavior in both the stresses and deformations as well as the diffusion process. We first look at a case where the fibers are transversely isotropic and the matrix is isotropic, but the diffusion parameters are the same. In the second case we consider the full complexity where the fibers and the matrix are different in all parameters.

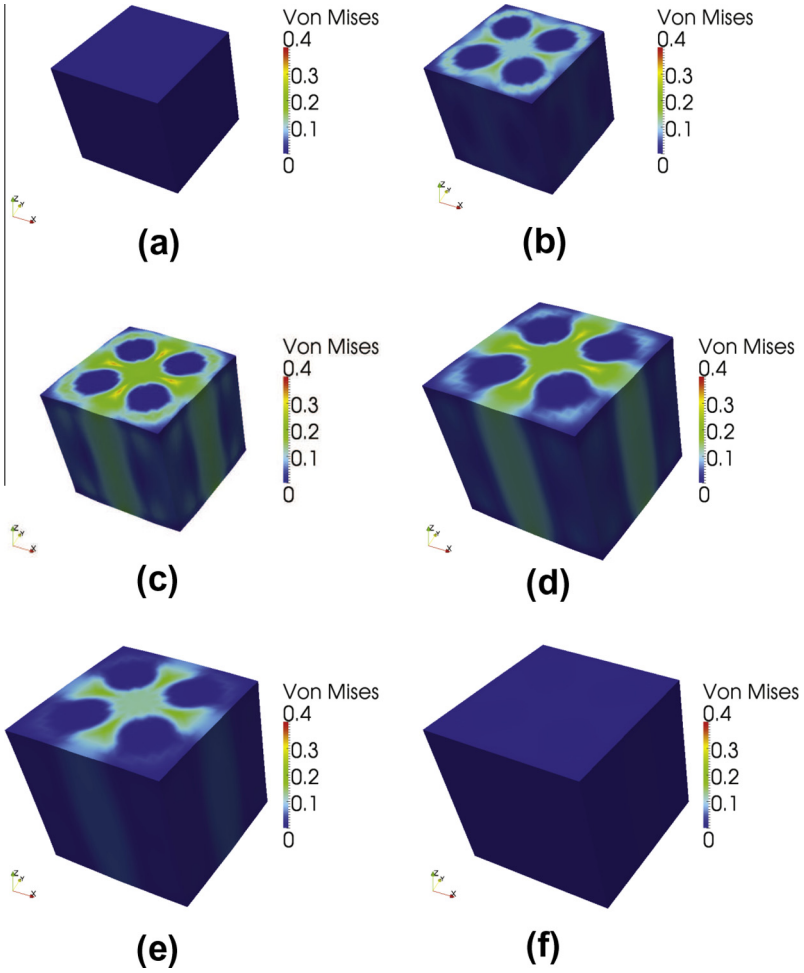

Fig. 9. Fiber composite swelling, case 2: plots of the Von Mises stress at different time steps (displacements are magnified by a factor of 200).

7.4.1. Case 2: strain dependent diffusivity

In this case four fibers are positioned in the matrix equally spaced. We consider the following constitutive models for both the fibers and the matrix:

$$\begin{aligned} \widetilde{\mathbf{D}} &= \widetilde{\mathbf{D}}_0 \frac{e^J - 1}{e - 1} \\ \mathbf{S} &= \mathbb{E} : \mathbf{E} - \beta(\widetilde{C} - \widetilde{C}_0)\mathbf{I} \end{aligned} \tag{31}$$

With an isotropic model for the matrix (Epoxy), and a transversely isotropic for the fibers (carbon-fibers). Fig. 9 displays the Von Mises stress in the block. During the transient phase we observe the different stresses that arise due to the spatial distribution of the concentration and the different mechanical stiffness of the matrix and the fibers. There is a stress concentration in the matrix in between the fibers as a result of that. As the distribution of the concentration in the block becomes homogeneous at steady state, the stress is reduced to zero. That is due to the fact that the strains-due-to-diffusion are modeled to be the same for both materials. For a homogeneous concentration the block swells and deforms in a homogeneous and isotropic manner. The mechanically-induced-strains become equal to the strains-due-to-diffusion and the stress is zero as a result. This example illustrates the freedom of this model, that has three different modeling possibilities: mechanical, diffusion, and the coupling of them.

7.4.2. Free swelling of a fiber composite with case 1 for the matrix and case 4 for the fibers

We now consider a more complex case that includes different models and characteristics for the fiber and the matrix, both in diffusion and mechanics. A more complex placement of the fibers in the matrix is considered to resemble a realistic fiber-composite material. The fibers are embedded in the matrix in different orientations with a 90° difference between the fiber bundles. For the matrix, we consider an isotropic material (Epoxy), and the following constitutive model for the diffusion:

$$\begin{aligned} \widetilde{\mathbf{D}} &= \widetilde{\mathbf{D}}_0 \\ \mathbf{S} &= \mathbb{E} : (\mathbf{E} - \beta(\widetilde{C} - \widetilde{C}_0)\mathbf{I}) \end{aligned} \tag{32}$$

and for the fibers, we consider a transversely-isotropic material (carbon-fibers) that does not elongate in the fiber direction due to diffusion:

$$\begin{aligned} \widetilde{\mathbf{D}} &= \widetilde{\mathbf{D}}_0 \\ \mathbf{S} &= \mathbb{E} : (\mathbf{E} - \beta(\widetilde{C} - \widetilde{C}_0)(\mathbf{I} - \mathbf{M} \otimes \mathbf{M})) \end{aligned} \tag{33}$$

where $\mathbf{M}$ is the fiber direction. As a result, the parameters and model for deformation-induced-by-diffusion are different for the matrix and the fibers. Fig. 10 shows how the non-dimensional Von Mises stress (divided by the yield stress), change during the change of concentration in the block. The heterogeneity of material in all

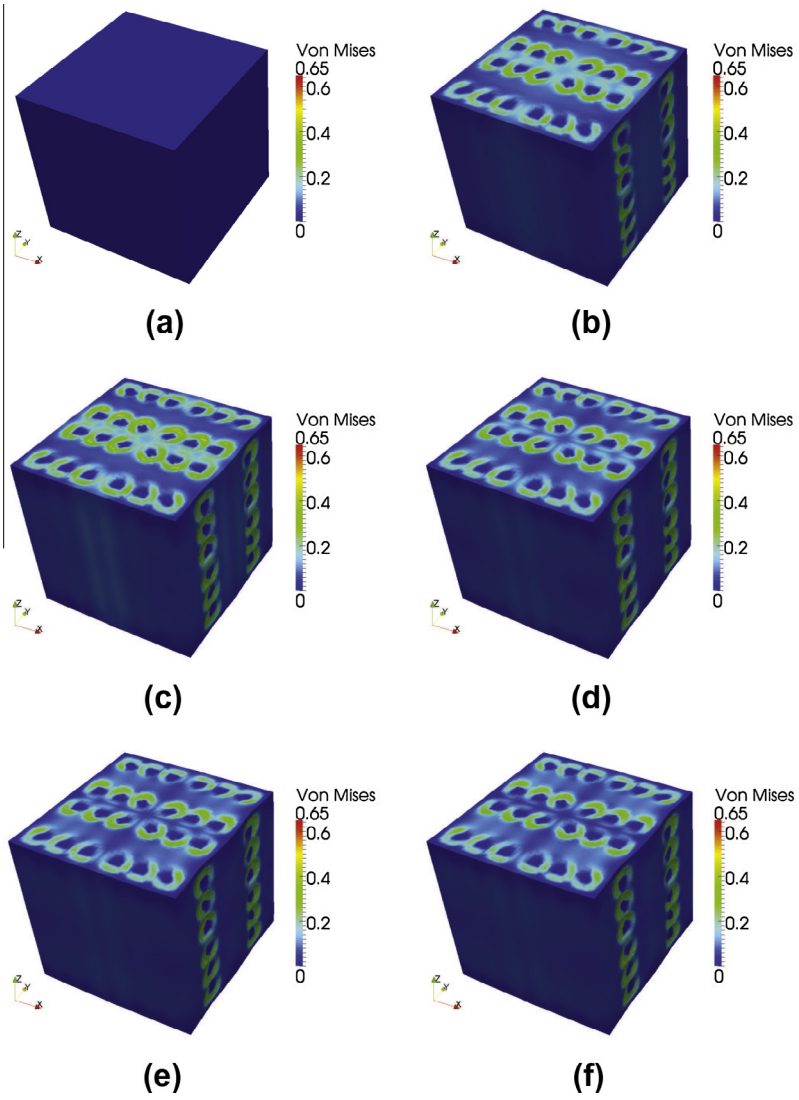

Fig. 10. Fiber composite swelling, cases 1 and 4: plots of the Von Mises stresses at different time steps (displacements are magnified by a factor of 200).

the parameters produces a steady state configuration that is not stress free. As the two materials act differently for the same levels of concentration stresses and deformations are not the same, causing stress concentrations where the fibers and the matrix are joined. The overall deformations are complex compared to the other cases shown here and depend on the orientation of the fibers as well.

In Fig. 11 the magnitude of the displacement change during the change of concentration is shown in one eighth of the body. The difference between the fibers and the matrix is most evident and the locations of the fibers plays a major role as well. The fibers close to the edges cause edge effects and deform in a different manner than fibers closer to the middle of the matrix. The center of the block does not deform, as expected, but the spherical isosurfaces are not apparent and the overall displacement is highly influenced by the fibers and the matrix.

The complexity of the stresses and deformations in fiber composite materials due to the coupling between diffusion and deformation can be fully appreciated in this case. This examples illustrates the full capacity of the models developed here, showing that if a fiber composite is considered to be used for diffusion, an analysis is required.

8. Summary

In this work, we developed a model for strongly-coupled, deformation-dependent diffusion in composite media at finite strains, which incorporates the effects of deformation into the diffusivity tensor. A time-transient three-dimensional variational formulation was developed and then discretized using the *Finite Element* method. The strong multiphysical coupling was resolved using a staggering scheme. A series of numerical examples were provided to investigate the mathematical model. The examples included complex scenarios that analyzed fiber-reinforced composite materials with different mechanical and diffusivity characteristics for the fibers and the matrix. In that case the simulations provided an insight into how the nonlinearity and strong coupling are effecting the stresses and deformations in a heterogeneous material due to the diffusion process. Specifically, three physically based main models were developed and simulated in free swelling: strain-dependent diffusivity, nonuniform diffusion-induced-strains, and saturation. These mathematical models and computational framework can be used to further study different combinations of fibers and matrix materials, and to optimize the parameters for best results. The utility of this model is the ability to streamline the

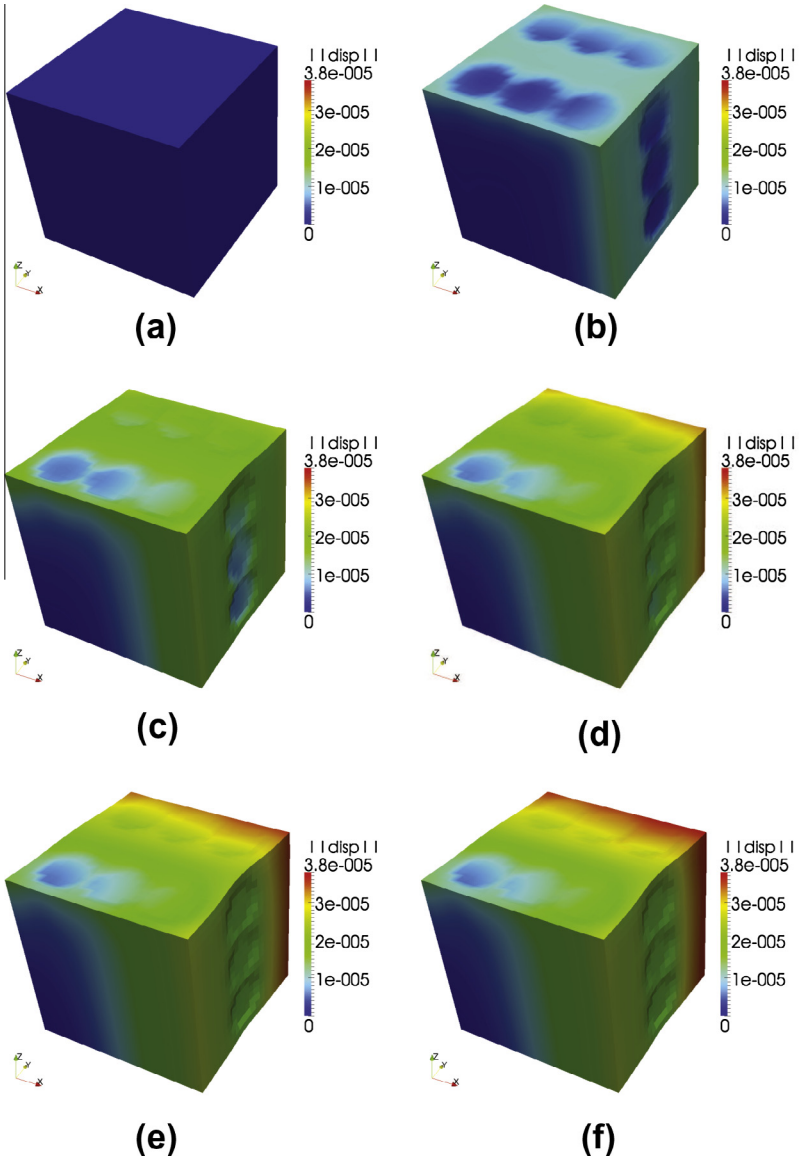

Fig. 11. Fiber composite swelling, cases 1 and 4: plots of the magnitude of the displacement at different time steps (displacements are magnified by a factor of 200). *Note*: only one eighth of the cube is plotted.

number of difficult and time-consuming experiments. The general framework developed allows for natural extensions to include other material models such as the Ogden family, Mooney–Rivlin and Blatz–Ko type models. This is under investigation by the authors.

References

[1] Truesdell C. Mechanical basis of diffusion. J Chem Phys 1962;37:2336–44.
[2] Green AE, Adkins JE. A contribution to the theory of non-linear diffusion. Arch Ration Mech Anal 1974;15(3):235–46.
[3] Adkins JE. Diffusion of fluids through aeolotropic highly elastic solids. Arch Ration Mech Anal 1964;15(3):222–34.
[4] Adkins JE. Non-linear diffusion III diffusion through isotropic highly elastic solids. Philos Trans Royal Soc Lond Series A, Mathe Phys Sci 1964;256(10):301–16.
[5] Unger DJ, Aifantis EC. On the theory of stress-assisted diffusion, II. Acta Mech 1983;47(1):117–51.
[6] Wilson RK, Aifantis EC. On the theory of stress-assisted diffusion, I. Acta Mech 1982;45(3):73–296.
[7] Aifantis EC. On the problem of diffusion in solids. Acta Mech 1980;37(3):265–96.
[8] Rajagopal KR. Diffusion through polymeric solids undergoing large deformations. Mater Sci Technol 2003;19(9):175–1180.
[9] Baek S, Srinivasa AR. Diffusion of a fluid through an elastic solid undergoing large deformation. Int J Non-Linear Mech 2004;39(2):01–218.
[10] Hong W, Zhao X, Zhou J, Suo Z. A theory of coupled diffusion and large deformation in polymeric gels. J Mech Phys Solids 2008;56(5):1779–93.
[11] Zohdi T. Modeling and simulation of a class of coupled thermo-chemo-mechanical processes in multiphase solids. Comput Methods Appl Mech Eng 2004;193(6–8):679–99.
[12] Duda FP, Barbosa JMA, Guimarães LJ, Souza AC, PEM-COPPE CU, de Janeiro RJ. Modeling of coupled deformation-diffusion-damage in elastic solids. Int J Model Simul Petrole Ind 2007;1(1).
[13] Hairer E, Nørsett S, Wanner G. Solving ordinary differential equations. I: Nonstiff problems. Springer; 1993.
[14] Hairer E, Wanner G. Solving ordinary differential equations II: Stiff and differential-algebraic problems, vol. 2. Springer; 2004.